Band-gap shift in heavily doped *n*-type $Al_{0.3}Ga_{0.7}As$ alloys

A. Ferreira da Silva
Instituto Nacional de Pesquisas Espaciais, INPE/LAS—C.P. 515, 12201-970 São José dos Campos, SP, Brazil

C. Persson
Linköping University, Department of Physics and Measurement Technology, S-58183 Linköping, Sweden

M. C. B. Marcussen and E. Veje
Oersted Laboratory, Niels Bohr Institute, Universitetsparken 5, DK-2100 Copenhagen, Denmark

A. G. de Oliveira
Departamento de Física—ICEX, Universidade Federal de Minas Gerais, 30123-970 Belo Horizonte, MG, Brazil
(Received 28 December 1998)

The band-gap shift of heavily Si-doped $Al_{0.3}Ga_{0.7}As$ alloys has been investigated theoretically and experimentally at low temperature. The calculations are carried out within a framework of the random phase approximation and the electron-electron, electron-optical phonon, and electron-ion interactions have been taken into consideration. The experimental data have been obtained with photoluminescence and photoluminescence excitation spectroscopy. Theoretical and experimental results fall closely together in a wide range of impurity concentration. [S0163-1829(99)02928-8]

I. INTRODUCTION

Owing to the technological applications in a variety of high-performance, modern optoelectronic devices, $Al_xGa_{1-x}As$ alloys have been extensively investigated recently.[1–20] Most of these investigations were directed towards the information extracted from the optical properties, such as, e.g., carrier effective masses, energy gap, donor and acceptor binding energies,[4,8,10–12,20] Hall measurements,[13] DX centers,[4,7,14] excitonic states,[15,16] dense electron-hole systems,[17] hydrostatic pressure,[18] and temperature dependence of the energy gap.[5] However, neither experimental nor theoretical efforts have been much devoted to investigate the band-gap shift (BGS), caused by heavy doping of $Al_xGa_{1-x}As$ alloys. Understanding the role of impurities is very important to semiconductor device technology. The efficiency of these devices is strongly affected by the incorporation of impurities and the variation of alloy composition as well. Experiments on doped semiconductors, above the impurity critical concentration N_c for the metal-nonmetal (MNM) transition (Mott transition), reveal a BGS beyond 10% of the band gap of the pure material.[21–30]

For an intrinsic or slightly doped semiconductor with direct band gap, there is one fundamental band-gap energy, namely, the separation in energy between the upper edge of the valence band and the lower edge of the conduction band. This energy can be determined experimentally from measurements based on photoabsorption. However, when donor atoms are introduced, the fundamental band gap is reduced at the same time as the position of the Fermi level above the top of the valence band increases, and for sufficiently doped samples, the Fermi level will fall above the conduction band edge. Then, the band gap seen in measurements based on photoabsorption becomes greater than the conduction band gap, which can be determined from emission measurements like photoluminescence (PL), as is done here. Traditionally, the former gap is called the optical band gap, whereas the latter gap is called the reduced band gap. For the determination of the former, photoluminescence excitation (PLE) measurements were carried out here. The band structure near the fundamental gap of a heavily doped *n*-type semiconductor, showing the reduced gap, the optical gap, and the Fermi level, is described in a very illustrative way in the fundamental work of Wagner on heavily doped silicon in Ref. 26.

We have investigated the BGS of the $Al_xGa_{1-x}As$ alloys as a function of both donor impurity concentration N and alloy composition x at low temperature, using the crystal parameters listed in Table I. Si is the dopant in the alloys. The applied calculation method is based on the random phase approximation (RPA), with a local field correction of Hubbard. In a model expounded by Berggren and Sernelius[21,22,28] the energy shift ΔE_g of the band gap is caused by the electron-electron and electron-ion interactions. Moreover, the Coulomb potential is screened by a frequency dependent lattice dielectric function, arising from electron-optical phonon interaction and scattering between valence and conduction-band states.

II. EXPERIMENTAL DETAILS AND CONSIDERATIONS

A. Sample production

The investigated uniformly doped $Al_xGa_{1-x}As$ samples with different silicon dopant concentrations were grown by molecular beam epitaxy (MBE) at 620 °C on semi-insulating [001]-oriented Cr-doped GaAs substrates with the following layer sequence: a 0.3-μm-thick undoped GaAs buffer, a 0.5-μm-thick undoped $Al_xGa_{1-x}As$ buffer, the active 3.0-μm-thick silicon-doped $Al_xGa_{1-x}As$ layer, and 60-Å-thick silicon-doped GaAs cap layer. The aluminum fraction, fixed

TABLE I. Low temperature values of the energy gap, effective masses, dielectric constants, lattice parameter, and phonon energy used in the calculation for $Al_xGa_{1-x}As$ at the Γ point of the Brillouin zone. The labels hh and lh mean heavy- and light-hole, respectively. Most of the values were extracted from Refs. 4, 19, and 33.

	$Al_xGa_{1-x}As$	$x=0.3$
Energy gap		
E_g (eV)	$1.5194+1.36x+0.22x^2$	1.947
Dielectric constants		
ϵ_0	$12.40-2.79x$	11.56
ϵ_∞	$10.60-2.73x$	9.78
Electron mass		
m_d/m_0	$0.0665+0.0835x$	0.0916
Hole masses		
m_{hh}/m_0	$0.51+0.20x$	0.570
m_{lh}/m_0	$0.082+0.078x$	0.105
m_h/m_0[a]	$0.53+0.23x$	0.60
Lattice parameter		
a (Å)	$5.6535+0.0087x$	5.6561
Phonon energy		
$\hbar W_{LO}$ (eV)		0.040

[a]Minority carrier density of states effective mass $m_h=(m_{hh}^{3/2}+m_{lh}^{3/2})^{2/3}$.

to 30% ($x=0.3$) for all samples, was measured by the reflection high energy electron diffraction (RHEED) technique.

B. Photoluminescence and photoluminescence excitation measurements

The measurements were carried out at the Copenhagen PL facility, which is described in detail in Refs. 5 and 31. In the present work, an argon ion laser (488 nm) was used as the light source for the measurements. The light emitted from the samples was dispersed in a 1 m optical spectrometer (McPherson model 2051), equipped with a 600-lines-per-mm grating blazed at 1000 nm, and it was detected with a cooled photomultiplier (Hamamatsu model R 943-02) using a personal-computer based single-photon counting technique. The overall relative quantum efficiency of the detecting device was determined by using a coiled-coil filament lamp standard of spectral irradiance (Optronic Laboratories model L-97), as described in Ref. 32. In the PLE measurements, a stabilized 250 W filament lamp coupled to a 0.67 m scanning monochromator (McPherson model 207) was used for illuminating the samples. The grating of the monochromator was blazed at 1000 nm and ruled with 600 lines-per-mm. The output photon fluence was determined on a relative scale as a function of the wavelength with the quantum-efficiency calibrated 1-m spectrometer used for the detection. In the PLE spectra, the data points were always normalized to the same number of photons used for excitation.

The samples were mounted in a closed-cycle helium refrigeration system which could operate between 10 K and room temperature. All experimental data presented here were taken at 10 K.

TABLE II. The first column gives the silicon concentration in the different samples, the next column presents the experimental values for the reduced band gap energy, and the corresponding values for the optical band gap energy are shown in the last column. The uncertainty related to each value given in the middle and the right columns are 20 meV or less.

Silicon concentration (10^{17} cm^{-3})	Reduced band-gap energy (eV)	Optical band-gap energy (eV)
2.0	1.89	1.91
5.8	1.86	1.88
16	1.83	1.85
60	1.75	1.82
100	1.64	1.82
200	1.51	1.81

C. Experimental data taking, treatment and results

The energy of the reduced band gap was derived from the PL spectra in the following way. In the spectra, the features related to the $Al_{0.3}Ga_{0.7}As$ layer could, for all samples, be separated from the PL related to the GaAs. For the samples of lowest Si concentration, the PL spectra were dominated by excitonic transitions, as described in Refs. 4 and 5, in which references to previous work can be found. Consequently, for these samples, the reduced band-gap energy for $Al_{0.3}Ga_{0.7}As$ was determined from the photon energy of the $Al_xGa_{1-x}As$–related excitonic radiative recombination, corrected for the exciton binding energy, which for $x=0.3$ is 6 meV (see Refs. 4, 5, and 19). For the more heavily doped samples, the PL spectra showed band-to-band radiative recombination, and the energy of the reduced band gap was determined from the low-energy limit of the PL feature related to the $Al_xGa_{1-x}As$. This procedure is very similar to that used by Wagner for heavily doped silicon, as described in Ref. 26. The experimental values for the reduced band gap as determined from the PL spectra are given in Table II. The overall uncertainty is estimated to be 20 meV or less.

PLE was carried out for detection wavelengths corresponding to all peaks with usable signal-to-noise ratios seen in PL. For transitions related to the $Al_xGa_{1-x}As$, the PLE signal, corrected for background, was extrapolated to zero level, and the threshold for photoexcitation determined this way was identified as the height of the optical band gap. This is a procedure very similar to that used in Ref. 26, except that no attention was paid here to phonon-assisted excitations, since the band gaps studied here are of a direct nature.

PLE was also carried out at detection wavelengths for transitions from the GaAs. In such cases, a PLE signal was also observed for excitation energies below the fundamental threshold for excitation in $Al_xGa_{1-x}As$, caused by photoexcitation in GaAs. However, it came out that this PLE signal was quite flat in the region of interest, so that the position in threshold for excitation in $Al_xGa_{1-x}As$ could be derived satisfyingly well. For each sample, the threshold position obtained at different detection wavelengths agreed within uncertainty limits. The experimental values for the optical band-gap energy, as deduced from our PLE measurements, are presented in Table II. The overall uncertainty is estimated to be 20 meV or less.

All data given in Table II have been taken at 10 K. The temperature variation of the band-gap energy for $Al_xGa_{1-x}As$ has been studied, and the change in energy, when the temperature is increased from 0 to 10 K, is below 1 meV, see Ref. 5. Therefore, within uncertainty limits, the data in Table II can be taken as representative for a sample temperature of 0 K.

III. BAND-GAP SHIFT CALCULATION

We have calculated both the reduced and optical band gaps as described below.

The reduced band gap is written as

$$E_{g.2}=E_{g.0}-\Delta E_g, \tag{1}$$

where $E_{g.0}$ is the band-gap energy for undoped material and ΔE_g is the doping induced BGS. The corresponding optical band gap is

$$E_{g.1}=E_{g.2}+\Delta E_I \quad I=F \text{ or BM}. \tag{2}$$

In Eq. (2), ΔE_F is the shift in Fermi energy due to population of free carriers in the conduction band and $\Delta E_{\rm BM}$ is the Burstein-Moss shift.[34,35] They are written as

$$\Delta E_F=\frac{\hbar^2 K_F^2}{2m_d}, \tag{3}$$

$$\Delta E_F=\frac{\hbar^2}{2m_d}(3\pi^2 N)^{2/3}. \tag{4}$$

In Eq. (3) $K_F=(3\pi^2 N/\nu)^{1/3}$, where ν is the number of conduction band minima. In our case $\nu=1$.

$$\Delta E_{\rm BM}=\frac{\hbar^2}{2m_{dh}}(3\pi^2 N)^{2/3}, \tag{5}$$

$$\Delta E_{\rm BM}=\Delta E_F\left(1+\frac{m_d}{m_h}\right), \tag{6}$$

where $1/m_{dh}=1/m_d+1/m_h$, m_d is the density of states effective mass of the majority carriers, and m_h is the density of states effective mass of the minority carriers. The shift of the band gap due to doping has contributions from both a shift of the conduction band, ΔE_c, and of the valence band ΔE_v, and it is written as

$$\Delta E_g=-\Delta E_c+\Delta E_v. \tag{7}$$

Normally, ΔE_c is a negative quantity and ΔE_v is a positive quantity, implying that both contributions reduce the band gap as follows:

$$\Delta E_c=\mathrm{Re}[\hbar\Sigma_c^{\rm ee}(o)+\hbar\Sigma_c^{\rm ei}(o)], \tag{8}$$

$$\Delta E_v=\mathrm{Re}[\hbar\Sigma_v^{\rm ee}(o)+\hbar\Sigma_v^{\rm ei}(o)], \tag{9}$$

where $\hbar\Sigma_{c,v}^{\rm ee}(o)$ and $\hbar\Sigma_{c,v}^{\rm ei}(o)$ are self-energies due to electron-electron (ee) and electron-impurity (ei) interaction at the conduction band (c) minimum and valence band (v) maximum, respectively.[21] They are written as

$$\hbar\Sigma_c^{\rm ee}(o)=-\int\frac{d^3q}{(2\pi)^3}\int_{-\infty}^{+\infty}\frac{dw}{2\pi i}\frac{V_q}{K(w)}\left\{\frac{G_c^o(\overline{q},w)}{\tilde{\in}(\overline{q},w)}+\frac{1}{2}\left(\frac{1}{w+E_c(\overline{q})/\hbar-i\delta}-\frac{1}{w-E_c(\overline{q})/\hbar+i\delta}\right)\right\}, \tag{10}$$

$$\hbar\Sigma_v^{\rm ee}(o)=-\int\frac{d^3q}{(2\pi)^3}\int_{-\infty}^{+\infty}\frac{dw}{2\pi i}\frac{V_q}{K(w)}\left(\frac{1}{\tilde{\in}(\overline{q},w)}-1\right). \tag{11}$$

$$\{\Lambda_{\rm hh,hh}G_{v,\rm hh}^o(\overline{q},w)+\Lambda_{\rm hh,lh}G_{v,\rm lh}^o(\overline{q},w)\},$$

$$\hbar\Sigma_c^{\rm ei}(o)=\frac{N}{\hbar}\int\frac{d^3q}{(2\pi)^3}\left(\frac{V_q}{K(o)}\frac{1}{\tilde{\in}(\overline{q},o)}\right)^2 G_c^o(\overline{q},o), \tag{12}$$

$$\hbar\Sigma_v^{\rm ei}(o)=\frac{N}{\hbar}\int\frac{d^3q}{(2\pi)^3}\left(\frac{V_q}{K(0)}\frac{1}{\tilde{\in}(q,o)}\right)^2\cdot\{\Lambda_{\rm hh,hh}G_{v,\rm hh}^o(\overline{q},o)+\Lambda_{\rm hh,lh}G_{v,\rm lh}^o(\overline{q},o)\}, \tag{13}$$

where $E_c(\overline{q})$ is the energy dispersion of the conduction band, G_c^o, $G_{v,\rm hh}^o$, and $G_{v,\rm lh}^o$ are the unperturbed Green functions for conduction band, valence heavy-hole band, and valence light-hole band, respectively.[21] $\Lambda_{\rm hh,hh}$ and $\Lambda_{\rm hh,lh}$ are the Bloch overlap integrals between heavy-hole and heavy-hole bands and between heavy-hole and light-hole bands respectively.[21] $V_q/K(w)=4\pi e^2/[q^2K(w)]$ is the screened Coulomb potential. It comprises the virtual transitions across the band gap and all electron-optical phonon scatterings. $K(w)$ is the frequency dependent lattice dielectric function,

$$\frac{1}{K(w)}=\frac{1}{\in_\infty}+\frac{(\in_0-\in_\infty)W_{\rm LO}}{2\in_0\in_\infty}\times\left\{\frac{1}{w-W_{\rm LO}+i\delta}-\frac{1}{w+W_{\rm LO}-i\delta}\right\}, \tag{14}$$

where $\hbar W_{\rm LO}$ is the optical phonon energy of the longitudinal mode. $\tilde{\in}(q,w)$ is the dielectric function for the electron gas in the conduction-band minimum. It is written as

$$\tilde{\in}(\overline{q},w)=1-\left(1-\frac{1}{2}\frac{q^2}{q^2+K_F^2}\right)\frac{V_q}{K(w)}\frac{2}{\hbar}\int\frac{d^3p}{(2\pi)^3}\times\int_{-\infty}^{+\infty}\frac{du}{2\pi i}G_c^o(\overline{p},u)G_c^o(\overline{p}+\overline{q},u+w). \tag{15}$$

The experimental and theoretical results for the optical and reduced band-gap energies as well as for the total BGS and the valence and conduction-band contributions are shown in Figs. 1 and 2, respectively. As seen from these figures, there is satisfyingly good agreement between theory and experiment.

IV. CONCLUSION

In summary, we have investigated the reduced and optical band gaps of $Al_{0.3}Ga_{0.7}As$ alloys with PL and PLE as well as

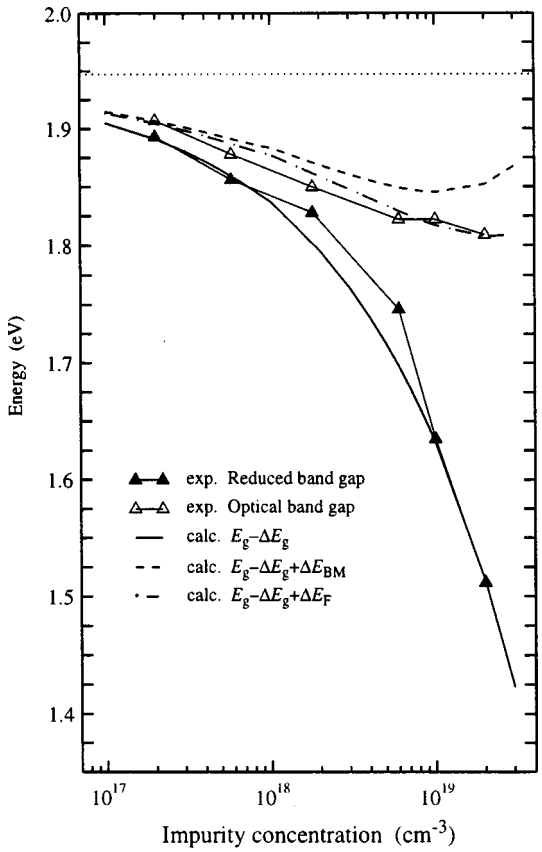

FIG. 1. Calculated and experimental band-gap energies for $Al_{0.3}Ga_{0.7}As$:Si as a function of impurity concentration. Dashed, dotted-dashed, and solid lines represent the calculated optical and reduced band-gap energies, respectively. Open triangles (optical gap) and filled triangles (reduced band gap) are the experimental data from the PL and PLE measurements. Dotted line represents the band-gap energy $E_{g.0}$ for undoped $Al_{0.3}Ga_{0.7}As$.

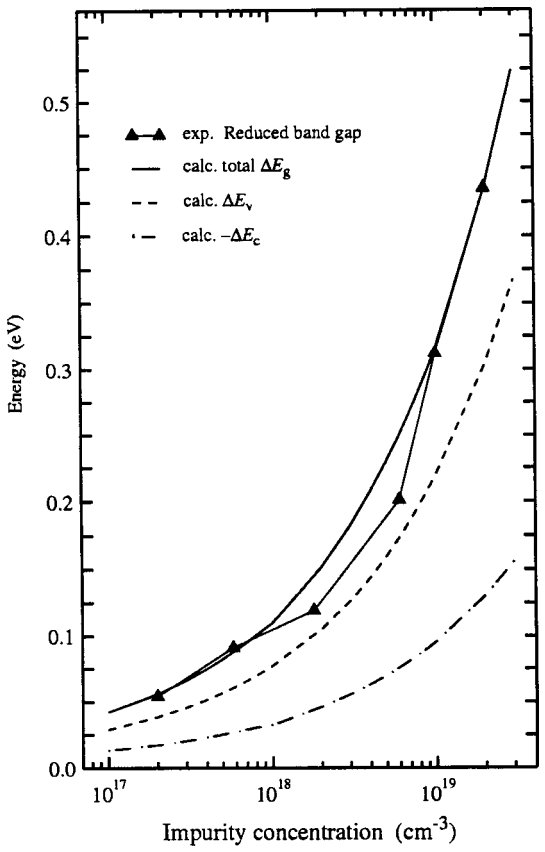

FIG. 2. Contributions to the total BGS, ΔE_g, in $Al_{0.3}Ga_{0.7}As$:Si as a function of impurity concentration. Solid triangles are the measured data. Solid line is the total ΔE_g. Dashed line is the upward of the valence band ΔE_v. Dotted-dashed line is the downward of the conduction band ΔE_c.

with a method based on the random phase approximation (RPA) with a local field correction of Hubbard. Experimental and theoretical results fall closely together in a wide range of impurity concentration. The contribution of the valence band has a major effect on the total BGS compared to the conduction band. It is worth mentioning that both the conduction and valence bands are considered to be parabolic, and in the analyses of experimental data the lifetime effects, Ref. 29, are not included.

ACKNOWLEDGMENTS

This work was financially supported by the Brazilian National Research Council (CNPq), the Swedish Research Council for Technical Sciences (TFR), the Danish Natural Science Research Council, the Carlsberg Foundation, Director Ib Henriksens Foundation, and the NOVO Nordic Foundation.

[1] A. Ferreira da Silva, C. Persson, K.-F. Berggren, I. Pepe, A. Santos Alves, and A. G. de Oliveira, Microelectron. Eng. **43-44**, 407 (1998).
[2] N. Galbiati, E. Grilli, M. Guzzi, P. Albertini, L. Brusaferri, L. Pavesi, M. Henini, and A. Gasparotto, Semicond. Sci. Technol. **12**, 555 (1997).
[3] T. Forchhammer, E. Veje, and P. Tidemand-Petersson, Phys. Rev. B **52**, 14 693 (1995).
[4] L. Pavesi and M. Guzzi, J. Appl. Phys. **75**, 4779 (1994).
[5] M. El Allali, C. B. Sorensen, E. Veje, and P. Tidemand-Petersson, Phys. Rev. B **48**, 4398 (1993).
[6] A. G. de Oliveira, G. A. M. Sáfar, and J. F. Sampaio, Braz. J. Phys. **24**, 363 (1994).
[7] J. F. Sampaio, A. S. Chaves, G. M. Ribeiro, P. S. S. Guimarães, R. P. de Carvalho, and A. G. de Oliveira, Phys. Rev. B **44**, 10 933 (1991).
[8] Y. Kajikawa, J. Appl. Phys. **69**, 1429 (1991).
[9] G. Borghs, K. Bhattacharyya, K. Deneffe, P. Van Mieghem, and R. Mertens, J. Appl. Phys. **66**, 4381 (1989).
[10] R. Dinngle, R. A. Logan, and J. R. Artur, Jr., Inst. Phys. Conf. Ser. **33a**, 210 (1977).
[11] M. O. Watanabe, K. Morizuka, M. Mashita, Y. Ashizawa, and Y. Zohta, Jpn. J. Appl. Phys., Part 2 **23**, L103 (1984).
[12] N. Galbiati, L. Pavesi, E. Grilli, M. Guzzi, and M. Henini, Appl. Phys. Lett. **69**, 4215 (1996).
[13] L. Pavesi, M. Henini, D. Johnston, and I. Harrison, Semicond. Sci. Technol. **10**, 49 (1995).

[14] G. Medeiros-Ribeiro, A. G. de Oliveira, G. M. Ribeiro, and D. A. W. Soares, J. Electron. Mater. **24**, 907 (1995).
[15] C. Bosio, J. L. Staehli, M. Guzzi, G. Burri, and R. A. Logan, Phys. Rev. B **38**, 3263 (1988).
[16] G. Torres-Delgado, R. Castanedo-Perez, P. Diaz-Arencibia, J. G. Mendoza-Alvarez, J. L. Orozco-Vilchis, M. Murillo-Lara, and A. Serra-Jones, J. Appl. Phys. **78**, 5090 (1995).
[17] H. Kalt and M. Rinker, Phys. Rev. B **45**, 1139 (1992).
[18] H. M. Cheong, J. H. Burnett, W. Paul, P. F. Hopkins, K. Campman, and A. C. Gossard, Phys. Rev. B **53**, 10 916 (1996).
[19] S. Adachi, J. Appl. Phys. **58**, R1 (1985).
[20] N. Chand, T. Hendersen, J. Klem, W. T. Masselink, R. Fischer, Y.-C. Chang, and H. Morkoç, Phys. Rev. B **30**, 4481 (1984).
[21] K. F.-Berggren and B. E. Sernelius, Phys. Rev. B **24**, 1971 (1981).
[22] K. F.-Berggren and B. E. Sernelius, Solid-State Electron. **28**, 11 (1985).
[23] S. C. Jain, J. M. McGregor, and D. J. Roulston, J. Appl. Phys. **68**, 3747 (1990).
[24] S. C. Jain and D. J. Roulston, Solid-State Electron. **34**, 453 (1991).
[25] S. C. Jain, R. P. Mertens, and R. J. Van Overstraeten, *Advances in Electronics and Electron Physics* (Academic, N.Y., 1991) Vol. 82, p. 197.
[26] J. Wagner, Phys. Rev. B **29**, 2002 (1984); **32**, 1323 (1985).
[27] J. Wagner and J. A. del Alamo, J. Appl. Phys. **63**, 425 (1988).
[28] B. E. Sernelius, Phys. Rev. B **36**, 4878 (1987).
[29] B. E. Sernelius, Inst. Phys. Conf. Ser. **91**, 153 (1987); Phys. Rev. B **34**, 5610 (1986).
[30] P. Nubile and A. Ferreira da Silva, Solid-State Electron. **41**, 121 (1997).
[31] O. K. Andersen and E. Veje, Phys. Rev. B **53**, 15 643 (1996).
[32] N. Andersen, K. Jensen, J. Jensen, J. Melskens, and E. Veje, Appl. Opt. **13**, 1965 (1974).
[33] *Numerical Data and Functional Relationships in Science and Technology*, edited by D. Madelung and M. Schulz, Landolt-Börnstein, New Series, Group III, Vol. 22, Part a (Springer, Berlin, 1987).
[34] E. Burstein, Phys. Rev. **93**, 632 (1954).
[35] T. M. Moss, Proc. Phys. Soc. London, Sect. B **67**, 775 (1954).